Temporal characteristics in nonequilibrium surface-growth models

Leonard M. Sander and Hong Yan
Randall Laboratory of Physics, University of Michigan, Ann Arbor, Michigan 48109-1120
(Received 15 April 1991)

We present analytical and numerical results showing $1/f^{\omega}$ characteristics in the time series of growth velocity in a class of surface-growth models. The exponent ω is found to be related to the scaling exponents by $\omega=(2\alpha-z+d-1)/z$. The time series of surface width in the steady state are also shown to have power-law scalings in the frequency domain. We establish a mapping between the single-step model for ballistic growth and a random cellular automaton. We conclude that the steady state of the surface-growth models, in particular the ballistic deposition model, is a self-organized critical state.

PACS number(s): 05.40.+j, 05.70.Ln, 68.35.Rh

I. INTRODUCTION

Self-similarities in space and time are ubiquitous in nature. In spatial organization, they are described by fractal geometry [1], while in the temporal domain, they are manifested by $1/f^{\omega}$ power spectra [2]. The comprehensive understanding of these phenomena, however, remains elusive. Recently, Bak, Tang, and Wiesenfeld (BTW) [3] have constructed a cellular automaton which, starting from an arbitrary initial state, evolves automatically into a unique critical state characterized by power-law correlations in both spatial and temporal scales. This intimate relation between the scale invariances in space and time resembles that of the critical state near a second-order phase transition. The fundamental difference here, however, is the lack of the external tuning parameters in the model (and in many systems in nature). Thus, this phenomenon is called "self-organized criticality" (SOC) by BTW. They argue that it is the achievement of this self-organized critical state that is responsible for the fractal structures and the $1/f$-type noise observed in nature.

On the other hand, in past years, there has been much development in studying nonequilibrium surface- (interface) growth problems [4]. Surface-growth processes are of great importance in a wide range of problems. Many models have been proposed to describe them, among them the Eden model for tumor growth [5] and the ballistic deposition model for vapor deposition [6]. Simulations of these models usually give rise to random rough surfaces whose roughness initially increases with time and then saturates. It is found, however, that these random surfaces have intriguing self-affine structures [7–10]. In the case of the ballistic deposition model [9,10], in which particles stick (to any of its neighbors) where they land on the surface, if one defines $s(\mathbf{r},t)=h(\mathbf{r},t)-h_0(t)$, where $h(\mathbf{r},t)$ is the height of the surface at position $\mathbf{r}$ and time t, and $h_0(t)$ is its spatial average, one gets

$$G(\mathbf{r}-\mathbf{r}',t-t')=\langle[s(\mathbf{r},t)-s(\mathbf{r}',t')]^2\rangle = |\mathbf{r}-\mathbf{r}'|^{2\alpha}F(|t-t'|/|\mathbf{r}-\mathbf{r}'|^{z}) . \quad (1.1)$$

Here $F(x)$ is a scaling function that is constant for $x \ll 1$ and approaches $x^{2\alpha/z}$ for $x \gg 1$ and $\langle\ \rangle$ denotes an ensemble average. The exponents α and z are characteristic quantities in the model considered and have the following interpretations: (i) correlations spread in the surface with rate $t^{1/z}$; (ii) the typical height difference at any given time is given by $\Delta s \simeq |\Delta \mathbf{r}|^{\alpha}$, with $\alpha<1$. This relation between the vertical scale and the lateral scale illustrates that the surface is a *self-affine fractal.*

An alternative scaling form of Family and Viscek [9] is that if we start at $t=0$ from a flat surface of length L, we have

$$\xi_L^2(t)=\frac{1}{L^{d-1}}\sum_{\mathbf{r}}[h(\mathbf{r},t)-h_0(t)]^2=L^{2\alpha}f(t/L^{z}) , \quad (1.2)$$

where ξ is the rms roughness of the surface (also called "surface width") averaged over the whole sample and over ensembles, and $d'=d-1$ is the substrate dimension in d-dimensional space. The scaling function $f(t/L^{z})$ is such that

$$\xi \simeq \begin{cases} t^{\alpha/z} & \text{if } t \ll L^{z} \\ L^{z} & \text{if } t \gg L^{z} . \end{cases} \quad (1.3)$$

It is widely believed that the essential physics of these models is captured by the continuum theory of Kardar, Parisi, and Zhang (KPZ) [11] in which they proposed an equation

$$\frac{\partial h}{\partial t}=\nu\nabla^2 h+\frac{\lambda}{2}(\nabla h)^2+D\eta \quad (1.4)$$

to describe the surface- (interface) growth processes. Here the first term on the right-hand side represents the relaxation of the surface by a surface tension ν, while the noise $\eta(\mathbf{r},t)$ in the last term is an uncorrelated white noise with Gaussian distribution and zero mean. The second term is attributed to the lateral growth. In the case of $\lambda=0$, the equation, which is linear, is the one originally put forward by Edwards and Wilkinson (EW) [12], and can be solved exactly. The result is $\alpha=\frac{1}{2}$ and $z=2$ for a one-dimensional substrate and $\alpha=0$ and $z=2$ for higher dimensions [in $2+1$ dimensions, this corresponds to a logarithmic scaling of the surface width, i.e., $\xi\simeq(\ln L)^{1/2}$, and in $3+1$ dimensions, a constant ξ].

When $\lambda \neq 0$, it means that flat surfaces grow at a different rate than sloped ones. For the ballistic deposition model, slopes grow faster than flat surfaces because of sticking on the sides. A scaling law [10] $\alpha+z=2$ is ensured by the Galilean invariance of the equation (1.4).

The self-affinity of the surface structures in these models is interesting. These models are very simple and accessible examples of time-dependent systems in which there is a kind of scale-invariant behavior automatically generated by the dynamical process. Therefore, it is natural to say that these systems exhibit SOC. In fact, as we shall see later, we can map the single-step model, a simplified version of the ballistic deposition model introduced by Meakin, Ramanlal, Sander, and Ball (MRSB) [10], onto a random cellular automaton whose growth rule is very similar to the avalanche rule in sandpile models [3]. On the other hand, however, it is easy to observe that the KPZ equation (1.4) does not contain a conserved deterministic dynamics, a condition regarded as crucial to achieve SOC in sandpile models [13–15], and there is no correspondence to avalanche events in these models. Nevertheless, it is important to investigate if these systems possess temporal $1/f$ characteristics and to understand its relevance to SOC. This is the purpose of our work.

In this paper, we will first establish a mapping that transforms the single-step model for ballistic growth into a random cellular automaton with simple growth rules. Then we will present numerical data as well as analytical results showing $1/f^{\omega}$ characteristic frequency spectra of the time series of growth velocity and surface width of the ballistic deposition model. The exponent ω is shown to be related to the scaling exponents α and z of the model in the case of growth velocity. The connection of these results to self-organized criticality will also be discussed followed by concluding remarks.

II. THE SINGLE-STEP MODEL AND MAPPING TO A CELLULAR AUTOMATION

The single-step model is illustrated in Fig. 1: we can imagine that atoms fall in straight lines randomly onto a surface. However, they can stick only at points where they can form bonds with all the neighbors in the level below. MRSB [10] mapped this model onto an Ising model in $1+1$ dimensions by setting $s(r)=h(r+\delta)-h(r)$. The dynamics is biased spin exchange, i.e., up spins can only move right, and down spins, left. In $2+1$ dimensions, they mapped the model to a (biased) six-vertex model. Plischke, Rácz, and Liu [16] considered an extension to allow evaporation as well as growth: this partly removes the bias in the spin exchange. Another, equivalent, visualization of the process, cf. Fig. 1, is in terms of "bricks" of length 2 that are allowed to fall onto the substrate at random points. They can only stick in local *minima* of the height $h(r)$, and convert a *minimum* to a *maximum*. This rule ensures that the height difference between a site and its neighbors can be ± 1 and nothing else. This restriction does not change the physics, but makes the mapping possible.

Here we introduce another mapping that emphasizes

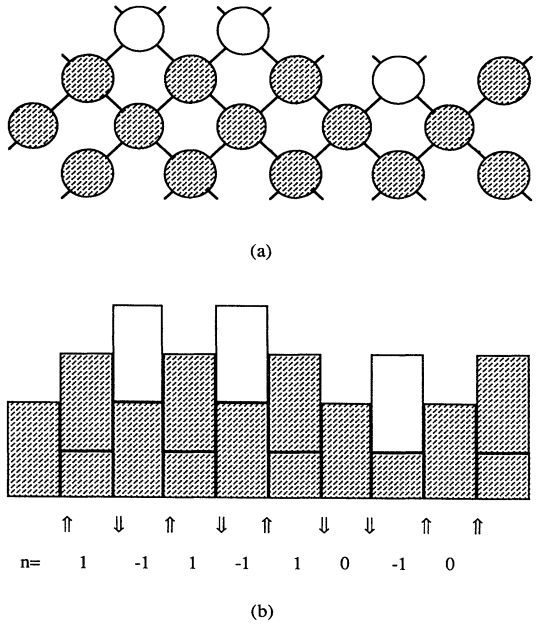

FIG. 1. (a) The single-step model in $1+1$ dimensions. Growth sites at the next step are shown by open circles. (b) An equivalent visualization of the model, with the mapping to a spin system, valid only in $1+1$ dimensions, and the n's for the current state.

the role of the height minima in the model. We always consider a hypercubic lattice, and we label each site by the number $n(r)$ as

$$n(r)=\tfrac{1}{2}\sum_{\delta}[h(r+\delta)-h(r)]\ , \tag{2.1}$$

where the sum is over the nearest neighbors. Thus a minimum carries a number $+d$, and the n's range between $-d$ and $+d$. The heights $h(r)$ are uniquely determined, up to an overall constant, by the n's: Eq. (2.1) is the (un-normalized) lattice Laplacian, thus the discrete Fourier transform of the n's is proportional to that of the h's. For small k,

$$n(k)\simeq k^2 h(k)\ . \tag{2.2}$$

Since

$$h(k,t)=\frac{1}{(L^{d'})^{1/2}}\sum_{r}[h(r,t)-h_0(t)]e^{ikr}\ , \tag{2.3}$$

following (1.3) we have

$$\langle h(k)h(-k)\rangle = k^{-d-2\alpha}F(k^z t,kL)\sim k^{-d-2\alpha},\quad t\gg L^z\ . \tag{2.4}$$

Thus the structure function of the n's and the exponent α is

$$S_n(k,t)=\langle n(k,t)n(-k,t)\rangle \simeq k^{4-d-2\alpha};\quad t\gg L^z\ . \tag{2.5}$$

The dynamics of the model is easily expressed in terms of the n's. We pick a site r at random, then if $n(r)\neq d$, we discard the move. Otherwise,

$$n(r)\rightarrow n(r)-2d\ ,$$
$$N(r\pm\delta)\rightarrow n(r\pm\delta)+1\ . \tag{2.6}$$

Equation (2.6) is almost exactly the same as the avalanche rules in models of sandpiles of BTW [3] and shares the same conservation law. (Here it is for local curvatures n rather than height h as in BTW models.) It should, however, be noted that there is no avalanche or dissipation occurring in the dynamic process discussed above, i.e., the system is "frozen" once the growth rule (2.6) is applied to a site and another site is chosen in the following step.

There are certain advantages of this mapping to that described in Ref. [10] (MRSB), namely that the generalization to $d>1$ is straightforward, and that the interpretation in terms of local geometry is useful. In Appendix A, we give a simple but complete proof of exact scaling $1+1$ dimensions based on this notion and examine some special features in higher dimensions, together with some numerical results.

III. $1/f^{\omega}$ NOISE IN THE TIME SERIES OF GROWTH VELOCITY

A. Analytical results

In surface-growth models, the growth velocity at site $\mathbf{r}$ and time t is

$$v(\mathbf{r},t)=\frac{\partial}{\partial t}h(\mathbf{r},t)\ . \tag{3.1}$$

Then

$$\langle v(\mathbf{r},t)v(\mathbf{r}',t')\rangle=\frac{\partial}{\partial t}\frac{\partial}{\partial t'}\langle h(\mathbf{r},t)h(\mathbf{r}',t')\rangle$$
$$=-\frac{1}{2}\frac{\partial}{\partial t}\frac{\partial}{\partial t'}\langle[h(\mathbf{r},t)-h(\mathbf{r}',h')]^2\rangle\ . \tag{3.2}$$

Letting $\bar{v}(\mathbf{r},t)=v(\mathbf{r},t)-v_0(t)$, where $v_0(t)$ is the spatial average of $v(\mathbf{r},t)$, from (1.1) we have

$$\langle\bar{v}(\mathbf{r},t)\bar{v}(\mathbf{r}',t')\rangle=-\frac{1}{2}\frac{\partial}{\partial t}\frac{\partial}{\partial t'}\langle[s(\mathbf{r},t)-s(\mathbf{r}',t')]^2\rangle$$
$$=\tfrac{1}{2}|\mathbf{r}-\mathbf{r}'|^{2(\alpha-z)}F''(|t-t'|/|\mathbf{r}-\mathbf{r}'|^z)\ , \tag{3.3}$$

where $F''(x)=\partial^2/\partial x^2F(x)$.

Now, averaging over $\mathbf{r}$ and $\mathbf{r}'$, we get

$$\langle\bar{v}(t)\bar{v}(t')\rangle=\frac{1}{2L^{2(d-1)}}\int\int d^{d-1}\mathbf{r}d^{d-1}\mathbf{r}'\cdot|\mathbf{r}-\mathbf{r}'|^{2(\alpha-z)}F''(|t-t'|/|\mathbf{r}-\mathbf{r}'|^z)$$
$$=\frac{1}{2L^{d-1}}\int d^{d-1}|\mathbf{r}-\mathbf{r}'|\cdot|\mathbf{r}-\mathbf{r}'|^{2(\alpha-z)}F''(|t-t'|/|\mathbf{r}-\mathbf{r}'|^z). \tag{3.4}$$

If $\tau=|t-t'|$, $r=|\mathbf{r}-\mathbf{r}'|$, and $y=r/\tau^{1/z}$, then

$$\langle\bar{v}(t)\bar{v}(t')\rangle=\frac{1}{2L^{d-1}}\int d^{d-1}rr^{2(\alpha-z)}F''(1/y^z)$$
$$=\frac{1}{2L^{d-1}}\tau^{[2(\alpha-z)+d-1]/z}$$
$$\times\int d^{d-1}yy^{2(\alpha-z)}F''(1/y^z)\ . \tag{3.5}$$

In large systems or on a small time scale, y tends to be very large, i.e., $1/y^z\ll 1$. As we pointed out in the Introduction, the scaling function F will approach a constant *plus* a correction to account for the finite size of real systems. This correction should be of an exponential form like $\simeq e^{-cr/L^z}$, where c is a constant. Therefore, the integral (3.5) is convergent, and we obtain

$$\langle\bar{v}(t)\bar{v}(t')\rangle\simeq\tau^{[2(\alpha-z)+d-1]/z}g(\tau/L^z)/L^{d-1}\ , \tag{3.6}$$

where $g(\tau/L^z)$ is a rapidly decaying function.

It is apparent that for $\tau/L^z\ll 1$, the velocity-velocity correlation follows a power law $1/\tau^{\gamma}$ with $\gamma=-[2(\alpha-z)+d-1]/z$. For $d=2$, i.e., growth on a one-dimensional substrate, $\alpha=\frac{1}{2}$, $z=\frac{3}{2}$, so $\gamma=\frac{2}{3}$. For $d=3$, there is not yet a commonly accepted value for exponent α, except that $\frac{1}{3}<\alpha<\frac{2}{5}$, thus $\frac{1}{4}<\gamma<\frac{2}{5}$. Note that in the Edwards-Wilkinson case, i.e., the weak-coupling phase in KPZ theory with $\lambda=0$, $z=2$, $\alpha=\frac{1}{2}$ (1+1 dimensions) or 0 (higher dimensions), therefore $\gamma=1$ in both $1+1$ and $2+1$ dimensions.

The Fourier transform of the velocity-velocity correlation (3.6) gives its frequency spectrum $V(f)$, which, ignoring the contribution from the exponential function, yields

$$V(f)\simeq\frac{1}{f^{\omega}}\ , \tag{3.7}$$

where

$$\omega=1-\gamma=\frac{2\alpha-z+d-1}{z}\ . \tag{3.8}$$

The function $g(\tau/L^z)$ in (3.6) will tend to bend the spectrum due to the convolution in the Fourier transform.

This result shows that, ideally, we should obtain a characteristic $1/f^{\omega}$ feature that is intrinsically related to the dynamical process of the system reflected in the

dependence of ω on the scaling exponents α and z. Notice, however, that $\omega=0$ for the Edwards-Wilkinson case in both $1+1$ and $2+1$ dimensions.

B. Numerical results

We have calculated the correlation function of growth velocities in the ballistic deposition model. In Fig. 2, we plot the v-v correlation function in $1+1$ dimensions for $L=1000$. We can see clearly that for a time period, the curve fits very well to $1/\tau^{2/3}$, while $(1/\tau^{2/3})e^{-\tau/750}$ fits the curve over almost the entire range of the time period we measure. This agrees with the analytical result of (3.6). The inset shows the same plot for the single-step model, which confirms that both models have the same scaling properties. Figure 3 presents the results in $2+1$ dimensions. We show here two curves with system sizes 100×100 and 75×75, respectively. Apparently, since we cannot go to larger systems in $2+1$ dimensions, the rapidly decaying function $g(\tau/L^z)$ has a significant effect here. Although g appears to be a more complicated function whose form is not yet known, we can fit the early part of the curves with a form $(1/\tau^{\gamma})e^{-\tau/\tau_0}$, where $\tau_0\simeq cL^z$. We get $\gamma=0.4$ for this fit, which is consistent with Eq. (3.8), though we cannot distinguish among the various values of α from different simulations. We can also see from Fig. 3 that the correlation extends further for larger systems. This fact indicates that the dropping edge in the graph is a size effect.

We then perform the Fourier transformation on the temporal correlation functions of the growth velocity. Figure 4 shows the frequency spectrum of the function plotted in Fig. 2. A function form $(1/f^{\omega})e^{-af}$ with $\omega=\frac{1}{3}$ appears to be a very good fit to the spectrum shown. The value of the exponent ω is exactly the value one would get according to Eq. (3.8). This is also the case in $2+1$ dimensions illustrated in Fig. 5, where we plot the frequency spectrum of the v-v correlation in Fig. 3 for system

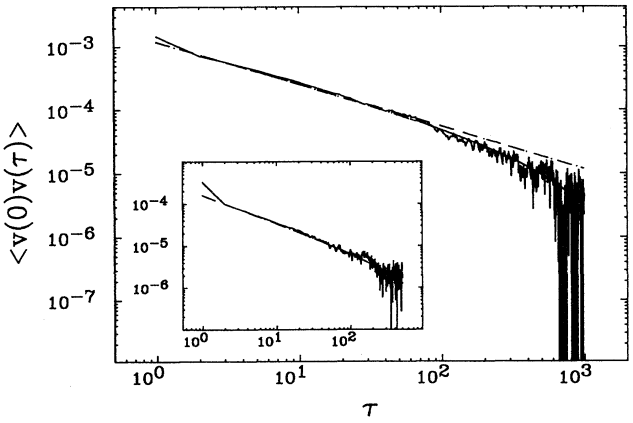

FIG. 2. The v-v correlation of the ballistic deposition model in $1+1$ dimensions. The graph is obtained for $L=1000$ averaged over 25 samples. The dashed straight line fit is $\sim1/\tau^{2/3}$, while another fit is $\sim(1/\tau^{2/3})e^{-\tau/750}$. In the inset is the v-v correlation of the single-step model. The fit is also $\sim(1/\tau^{2/3})e^{-\tau/750}$.

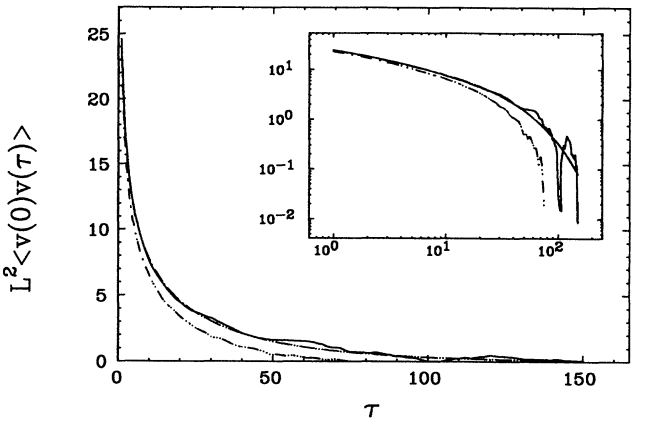

FIG. 3. The v-v correlations of the ballistic deposition model ($p=1$) in $2+1$ dimensions. The solid curve is for system size 100×100 and the dot-dashed curves is for 75×75, both averaged over 30 samples. The fit is $\sim(1/\tau^{0.4})e^{-t/40}$. The inset shows the same plot in a log-log scale.

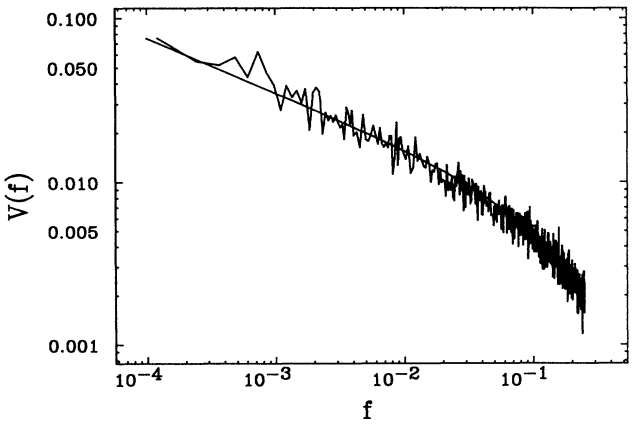

FIG. 4. The frequency spectrum of the v-v correlation in Fig. 2. The fit to the curve is $\sim1/f^{1/3}e^{-5f}$.

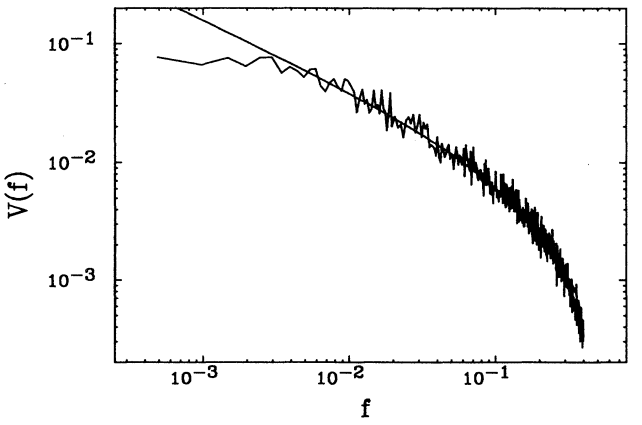

FIG. 5. The frequency spectrum of the v-v correlation in Fig. 3 for the 100×100 lattice. The fit to the curve is $\sim(1/f^{0.6})e^{-5f}$.

size 100×100. We obtain here $\omega=0.6$. Once again, we have a fairly good agreement with the analysis in Sec. III A. Note that the effect of $g(\tau/L^z)$ in (3.6) is significant, especially in the frequency spectra due to the finite-size effect, as shown in the graphs. In order to obtain the exponent, we used an exponential form $e^{-a\tau}$ to mimic the early behavior of g. However, we should point out that $e^{-a\tau}$ is not an exact form for $g(\tau/L^z)$. It fails to fit the high-frequency end of the spectrum, as well as sometimes the low end.

We have also carried out simulations on a modified ballistic deposition model of Yan, Kessler, and Sander (YKS) [17] that interpolates between the ballistic deposition model and the Edwards-Wilkinson model. There is a tuning parameter p in the model for which $p=1$ corresponds to the original ballistic deposition model, while $p=0$ corresponds to the Edwards-Wilkinson model. It was proposed that between $p=0.2$ and 0.4 there could be a phase transition, or possibly a slow crossover. We intend to check if there is a change in the scaling of the v-v correlations around the alleged phase-transition point. In Fig. 6, we plot the v-v correlations for both $p=0.4$ and 0.2 with system size 100×100. For $p=0.4$, we are able to fit the curve with exponent $\gamma=0.4$, which indicates that it follows the strong-coupling phase scaling law as in $p=1$ shown in Fig. 3. However, for $p=0.2$, it exhibits obvious deviation in scaling from that of $p=1$ and 0.4. A fit to the curve gives $\gamma=0.8$. This value is close to 1 as for $p=0$, and away from $\gamma=0.4$ for the strong-coupling phase. Notice also from both Figs. 3 and 6 that the v-v correlation for $p=0.4$ extends further than that of both $p=1$ and 0.2, a fact that is also reflected in the decay time τ_0 in $e^{-\tau/\tau_0}$. This observation is puzzling but is consistent with an ensemble fluctuation analysis [18], where it is found that the ensemble fluctuations in the steady state have a peak around the proposed phase-transition point. This may imply that there is another characteristic time scale other than L^z that plays an important role in the phase transition should the transition exist.

For the EW model, theoretical analysis suggests that $\omega=0$. Simulations in both $1+1$ and $2+1$ dimensions have confirmed this prediction. We note that since the ballistic deposition model represents a biased (thus driven) system, as is evident in the single-step model described in Sec. II, its temporal characteristics show $1/f$-type behavior, as in other driven systems [19]. However, for the EW model, it is a pure diffusive system without an external driving force except for a zero-mean random noise. So even though the system does possess long-range correlations both in time and space, it does not have a $1/f$-type frequency spectrum.

IV. TEMPORAL CHARACTERISTICS IN THE STEADY-STATE TIME SERIES OF SURFACE WIDTH

We have also examined the temporal characteristics of the time series of the surface width. The surface width $\xi(t)$ is defined in Eq. (1.2). In the steady state $t\gg L^z$, and $\xi(t)$ saturates and fluctuates around a constant that scales as L^α. It is interesting to investigate the fluctuations and correlations in this time series. Unfortunately, the analysis of this sequence involves four-point correlation functions that have unknown scaling properties. This complexity prevents us from doing the kind of straightforward analysis in the v-v correlations here. However, in the case of $\lambda=0$ in Eq. (1.4), the model is exactly solvable, so we are able to carry out calculations in this particular case that could shed some light on the subject. The analysis for the linear model is presented in Appendix B, whose results can be summarized here as $P(f)\simeq1/f^2$ in $1+1$ dimensions and $P(f)\simeq(a+b\ln f)/f^2$ in $2+1$ dimensions, where $P(f)$ is the power spectrum of the times series $\xi^2(t)$.

Figure 7 shows the correlations in the time sequences

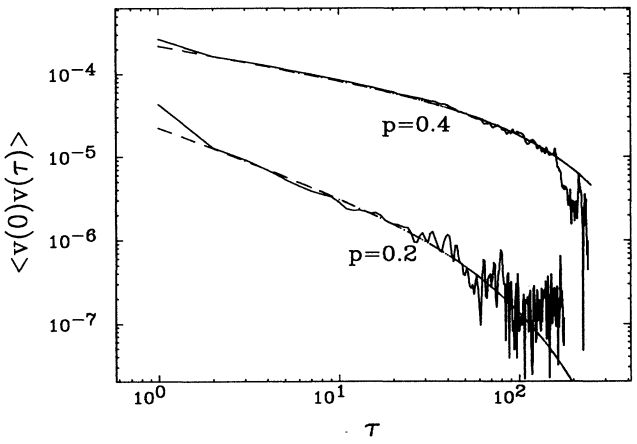

FIG. 6. The v-v correlations of $p=0.4$ and 0.2 for system size 100×100 and averaged over 30 samples. The fit to the curve of $p=0.4$ is $\sim(1/\tau^{0.4})e^{-\tau/150}$, and the fit to that of $p=0.2$ is $\sim(1/\tau^{0.8})e^{-\tau/70}$.

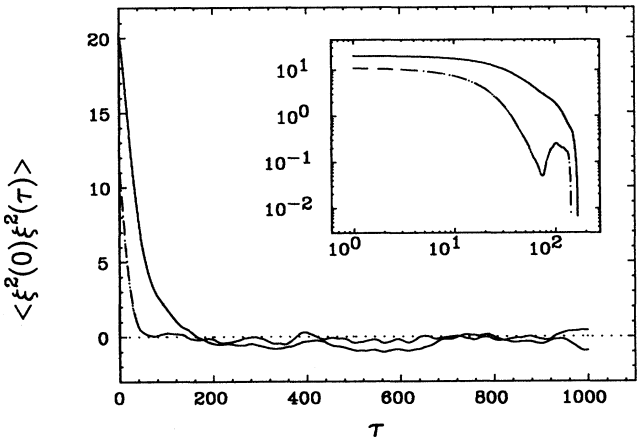

FIG. 7. The correlations in the time sequences of squared surface width in a $(2+1)$-dimensional ballistic deposition model ($p=1$). The solid line is for system size 100×100 and the dashed line is for 60×60, all averaged over 25 samples. The inset shows the same plot in a log-log scale.

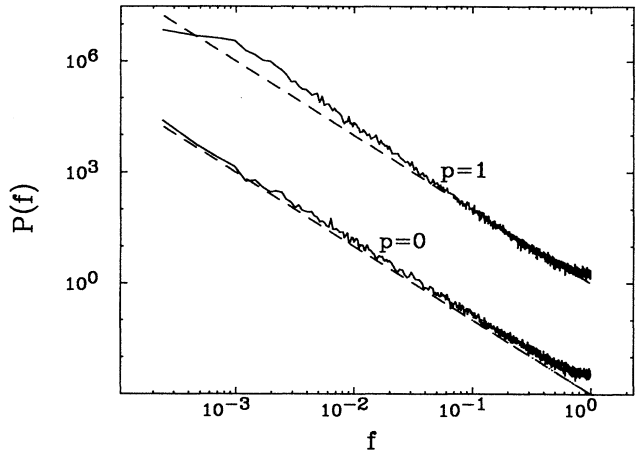

FIG. 8. The power spectra of the correlations in the time sequences of squared surface width in 1+1 dimensions for $p=1$ and 0 with $L=100$. The dashed lines are $\sim 1/f^2$.

in a (2+1)-dimensional ballistic deposition model. Different plots correspond to different system sizes. The correlations decrease in time rather slowly, as shown in the log-log plot in the inset. For larger system sizes, the correlations would extend over longer periods of time, which is evident in the graph.

The power spectra of these time series are plotted in Fig. 8, (1+1 dimensions) and Fig. 9 (2+1 dimensions). Both spectra of ballistic deposition ($p=1$ in the YKS model) and the EW model ($p=0$) are shown. In Fig. 8, both curves scale as $1/f^{\omega}$, with $\omega \geq 2$. While $1/f^2$ fits the curve of $p=0$ as predicted, the exponent ω for $p=1$ is clearly larger than 2; in fact, $\omega \simeq 2.25$. For 2+1 dimensions, as shown in Fig. 9, the curve of $p=0$ can be fitted by the predicted form $[a+b\ln(f)]/f^2$ very well, with $a=0.015$ and $b=0.0019$. For the ballistic deposition

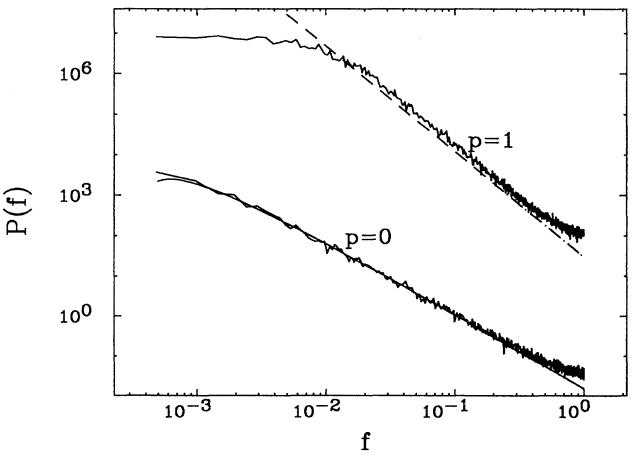

FIG. 9. The power spectra of the correlations in the time sequences of squared surface width in 2+1 dimensions for $p=1$ and 0 with lattice size 100×100. The fit to the curve of $p=1$ is $30/f^{2.6}$, while the fit to the curve of $p=0$ is $[0.015+0.0019\ln(f)]/f^2$.

model, a power-law fitting gives $\omega=2.6$. We do not have an explanation for these results.

V. DISCUSSION AND CONCLUSIONS

In the previous sections, numerical results as well as analytical analysis show that, in addition to their spatial scale invariance, surface-growth models, in particular the ballistic deposition model, have long-range temporal correlations as well. This fact illustrates that for this class of nonequilibrium surface-growth models, systems evolve through their own dynamical processes to a state with all the expected properties of a self-organized critical state. However, these systems are different from sandpile models [13,15], where the conserved dynamics is essential to achieve SOC. For the systems discussed here, the role of the conservation law is ambiguous, because from the KPZ equation (1.4), the dynamics of the height variable h is apparently not conserved, whereas the dynamics of the local curvature is nevertheless a conserved parameter, as shown in the mapping (2.6). As pointed out by Hwa [19], conservation laws in general are not necessary for the occurrence of SOC; other symmetries, like the translational invariance present in the KPZ equation in this case, can also induce long-range correlations in both time and space. Note that even though there are no avalanches here, correlations propagate throughout the system via diffusion and lateral interactions. On the other hand, the mapping we have established between the single-step model and the sandpile model reveals curious similarities in some aspects of the dynamics in both systems.

In conclusion, we have presented analytical as well as numerical results to show that the steady state of the ballistic deposition model (thus of other models in the same universality class) appears to be a SOC state in which the temporal characteristics of the growth velocity have long-range correlations and show $1/f^{\omega}$ behavior. The exponent ω has been shown to be related to the scaling exponents α and z, thus intrinsic to the system dynamics.

ACKNOWLEDGMENTS

We should like to thank David Kessler for numerous discussions during the course of this work. We acknowledge useful conversations with C. Caroli, L.-H. Tang, and D. Wolf. L.M.S. would like to thank the GPS at Université Paris VII for hospitality while part of this work was done. This work is supported by NSF Grant No. DMR88-15908. Computing funds are provided by the NSF San Diego Supercomputer Center.

APPENDIX A

We now give a complete proof of the exact scaling in 1+1 dimensions. The proof is, in fact, a clarification of the argument of MRSB [10], but in a way that makes the special role of the one-dimensional substrate completely transparent.

Consider the master equation for the probability

$P(\{n\},t)$ to be in a given configuration of n's at a given time:

$$\frac{dP(\{n\},t)}{dt} = \sum_{\{n'\}} W\{n' \to n\} P(\{n'\},t) - \sum_{\{n'\}} W\{n \to n'\} P(\{n\},t) . \quad \text{(A1)}$$

If we think of this as a matrix equation in which the P's are vectors with an entry for each configuration, then the first term is the off-diagonal process of creating the configuration, and the second is diagonal. There is an entry of one off diagonal element in the matrix for every process that leads to the given surface. But since every maximum in the configuration corresponds to a minimum in the parent, the number of off-diagonal elements is the number of maxima. The diagonal element is the number of minima.

In 1+1 dimensions, the number of minima is always equal to the number of maxima. Since the sum of each row of the matrix is zero, the steady state (the eigenvector with eigenvalue zero) has equal probability for all configurations. This is identical to the equilibrium state of the infinite-temperature Ising model, in which there are no spin correlations. Now note that since $n(r)=\frac{1}{2}[s(r)-s(r-\delta)]$, as is trivially obtained from Sec. II, we must have, for small k, $n(k)\sim ks(k)$. Thus

$$S_n = \langle n(k)n(-k)\rangle \simeq k^2 \langle s(k)s(-k)\rangle \simeq k^2 . \quad \text{(A2)}$$

The last step follows from the fact that $\langle s(r)s(r')\rangle = \delta_{rr'}$. From Eq. (2.5) we have $\alpha=\frac{1}{2}$.

In higher dimensions, it is not necessarily true that the number of minima is equal to the number of maxima. The fundamental reason is that the constraints of global topology for $d \geq 2$ are much weaker than for $d=1$. For example, for $d=2$, the only relevant constraint for a function on a torus is that there must be at least one minimum and one maximum. In Fig. 10, we illustrate this point by showing numerical results on concentrations of elements in a configuration in 2+1 dimensions. Here $m_i = N_i / L^d$ is the concentration and N_i is the total number of each element in the configuration.

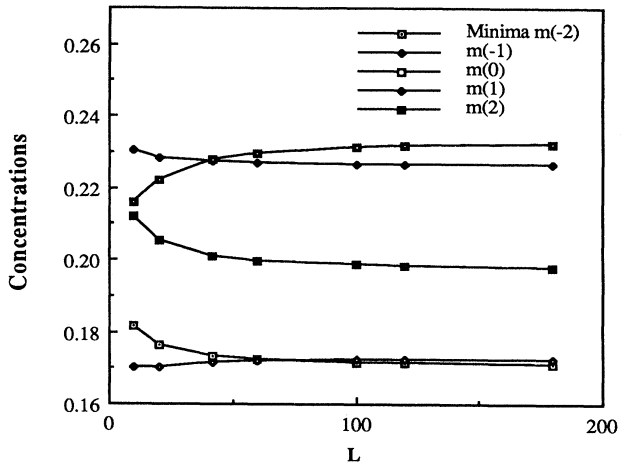

FIG. 10. The concentration of the various possible local geometries for various size lattices in 2+1 dimensions. The results were obtained in the steady state by averaging over approximately ten realizations. The statistical errors (obtained from the spread in the values among different realizations) are about the size of the symbols in the graph.

APPENDIX B

For the linear model, in a moving frame, the correlation function of the time series $\xi^2(t)$ is

$$S(t,s) = \int\int d\mathbf{x}\, d\mathbf{y} \langle h^2(\mathbf{x},t) h^2(\mathbf{y},s)\rangle = \sum_{\mathbf{k},\mathbf{q}} \langle |h(\mathbf{k},t)|^2 |h(\mathbf{q},s)|^2 \rangle . \quad \text{(B1)}$$

We know that

$$h(\mathbf{k},t) = G_0(\mathbf{k},t)h(\mathbf{k},0) + \int_0^t d\tau G_0(\mathbf{k},t-\tau)\eta(\mathbf{k},\tau) , \quad \text{(B2)}$$

where $G_0(\mathbf{k},t) = e^{-\nu k^2 t}\Theta(t)$ is the free propagator of the linear model where $\Theta(t)$ is a step function. Assuming flat substrate at $t=0$, $h(\mathbf{k},0)=0$. Thus

$$|h(\mathbf{k},t)|^2 = e^{-2\nu k^2 t} \int_0^t d\tau_1 \int_0^t d\tau_2 e^{\nu k^2(\tau_1=\tau_2)} \times \eta(\mathbf{k},\tau_1)\eta(-\mathbf{k},\tau_2) . \quad \text{(B3)}$$

Putting (B3) into (B1), we have

$$S(t,s) = \sum_{k,q} e^{-2\nu k^2 t} e^{-2\nu q^2 s} \int_0^t d\tau_1 \int_0^t d\tau_2 \int_0^s d\sigma_1 \int_0^s d\sigma_2 e^{\nu k^2(\tau_1+\tau_2)} e^{\nu q^2(\sigma_1+\sigma_2)} \langle \eta(k,\tau_1)\eta(-k,\tau_2)\eta(q,\sigma_1)\eta(-q,\sigma_2)\rangle . \quad \text{(B4)}$$

Here we omit the boldface notation for vectors. By applying the fact that the noise $\eta(k,t)$ is uncorrelated and assuming that $t > s$ without losing generality, we arrive at

$$S(t,s) = \left[\sum_k e^{-2\nu k^2 t} \int_0^t d\tau e^{2\nu k^2 \tau} \right]^2 + 2 \sum_k e^{-2\nu k^2 (t+s)} \int_0^s d\tau_1 \int_0^s d\tau_2 e^{2\nu k^2(\tau_1+\tau_2)} . \quad \text{(B5)}$$

Since we are interested in the steady state where $t \gg L^z$, we have $k^2 t \gg 1$ and $k^2 s \gg 1$, thus

$$S(t,s)=\left[\sum_k \frac{1}{2\nu k^2}\right]^2+\frac{1}{2\nu^2}\sum_k \frac{1}{k^4}e^{-2\nu k^2(t-s)}=S(\tau), \tag{B6}$$

where $\tau=t-s$.

The frequency spectrum of $S(\tau)$ is then

$$\begin{aligned}S(\omega)\int S(\tau)e^{i\omega\tau}d\tau &= c_d(L)\delta(\omega)+\frac{1}{2\nu^2}\left[\frac{L}{2\pi}\right]^{d-1}\int d\tau\, e^{i\omega\tau}\int_{l/L}^{\infty} d^{d-1}k\frac{e^{-2\nu k^2\tau}}{k^4}\\ &= c_d(L)\delta(\omega)+\frac{1}{2\nu^2}\left[\frac{L}{2\pi}\right]^{d-1}\int_{1/L}^{\infty} dk\frac{k^{d-6}}{i\omega-2\nu k^2}\ ,\end{aligned} \tag{B7}$$

where $\omega=2\pi f$ and $c_d(L)$ is a constant corresponding to the first term in (B6), which depends on dimensionality d and system size L. Assuming $x^2=2\nu k^2/\omega$ the real part of $S(\omega)$

$$\begin{aligned}\mathcal{R}(S(\omega)) &= c_d(L)\delta(\omega)+\frac{1}{\nu}\left[\frac{L}{2\pi}\right]^{d-1}\int_{1/L}^{\infty} dk\frac{k^{d-4}}{4\nu^2k^4+\omega^2}\\ &= c_d(L)\delta(\omega)+\frac{1}{\nu\omega^2}\left[\frac{L}{2\pi}\right]^{d-1}\left[\frac{\omega}{2\nu}\right]^{d-3/2}\\ &\quad\times\int_{(1/L)\sqrt{2\nu/\omega}}^{\infty} dx\frac{x^{d-4}}{1+x^4}\ .\end{aligned} \tag{B8}$$

In $1+1$ dimensions, $d=2$, so aside from the δ function at $f=0$ we have

$$\begin{aligned}S_{\rm re}(\omega) &\simeq \left[\frac{L}{2\pi}\right]\left[\frac{1}{\nu\omega^2}\right]\left[\frac{\omega}{2\nu}\right]^{-1/2}\\ &\quad\times\int_{(1/L)\sqrt{2\nu/\omega}}^{\infty}\frac{dx}{x^2(1+x^4)}\\ &\simeq \left[\frac{L}{2\pi}\right]\left[\frac{1}{\nu\omega^2}\right]\left[\frac{\omega}{2\nu}\right]^{-1/2}\frac{1}{(l/L)\sqrt{2\nu/\omega}}\\ &\simeq \frac{L^2}{2\pi\nu}\frac{1}{\omega^2}\simeq\frac{1}{\omega^2}\ .\end{aligned} \tag{B9}$$

For $d=3$,

$$\begin{aligned}S_{\rm re}(\omega) &\simeq \left[\frac{L}{2\pi}\right]^2\left[\frac{1}{\nu\omega^2}\right]\int_{(1/L)\sqrt{2\nu/\omega}}^{\infty}\frac{dx}{x(1+x^4)}\\ &\simeq -\left[\frac{L}{2\pi}\right]^2\left[\frac{1}{\nu\omega^2}\right]\ln\left[\frac{1}{L}\left[\frac{2\nu}{\omega}\right]^{1/2}\right]\\ &\simeq \frac{a+b\ln\omega}{\omega^2}\ ,\end{aligned} \tag{B10}$$

where a and b are constants.

[1] B. Mandelbrot, *The Fractal Geometry of Nature* (Freeman, San Francisco, 1982).

[2] See, e.g., P. Dutta and P. M. Horn, Rev. Mod. Phys. **53**, 497 (1981); W. H. Press, Comments Mod. Phys. C **7**, 103 (1978).

[3] P. Bak, C. Tang, and K. Wiesenfeld, Phys. Rev. Lett. **59**, 381 (1987); Phys. Rev. A **38**, 364 (1988).

[4] For the most recent reviews, see the articles by L. M. Sander and by J. Krug and H. Spohn in *Solids Far From Equilibrium: Growth, Morphology and Defects,* edited by Claude Godrèche (Cambridge University Press, Cambridge, England, in press).

[5] M. Eden, in *Proceedings of the 4th Berkeley Symposium on Mathematical Statistics and Probability,* edited by F. Neyman (University of California, Berkeley, 1961), Vol. IV.

[6] H. J. Leamy, G. H. Gilmer, and A. G. Dirks, in *Current Topics in Materials Science,* edited by E. Kaldis (North-Holland, Amsterdam, 1980), Vol. 6.

[7] M. Plischke and Z. Ràcz, Phys. Rev. Lett. **53**, 415 (1984).

[8] D. E. Wolf and J. Kertész, Europhys. Lett. **4**, 651 (1987).

[9] F. Family and T. Vicsek, J. Phys. A **18**, L75 (1985).

[10] P. Meakin, P. Ramanlal, L. M. Sander, and R. C. Ball, Phys. Rev. A **34**, 5091 (1986).

[11] M. Kardar, G. Parisi, and Y.-C. Zhang, Phys. Rev. Lett. **56**, 889 (1986).

[12] S. F. Edwards and D. R. Wilkinson, Proc. R. Soc. London Ser. A **381**, 17 (1982).

[13] T. Hwa and M. Kardar, Phys. Rev. Lett. **62**, 1813 (1989).

[14] P. L. Garrido, J. L. Lebowitz, C. Maes, and H. Spohn, Phys. Rev. A **42**, 1954 (1990).

[15] G. Grinstein, D-H. Lee, and S. Sachdev, Phys. Rev. Lett. **64**, 1927 (1990).

[16] M. Plischke, Z. Rácz, and D. Liu, Phys. Rev. B **35**, 3485 (1987).

[17] H. Yan, D. Kessler, and L. Sander, Phys. Rev. Lett. **64**, 926 (1990).

[18] H. Yan, D. Kessler, and L. Sander, J. Phys. A (to be published).

[19] T. Hwa, Ph.D. thesis, MIT, 1990.